

(1978).

⁵P. Estabrooks *et al.*, Nucl. Phys. **B133**, 490 (1978).⁶C. Sorensen, private communication.⁷M. B. Einhorn and C. Quigg, Phys. Rev. D **12**, 2015 (1975).⁸R. L. Kingsley, S. B. Treiman, F. Wilczek, and A. Zee, Phys. Rev. D **11**, 1919 (1975).⁹J. F. Donoghue and L. Wolfenstein, Phys. Rev. D **15**, 3341 (1977).¹⁰Harry J. Lipkin, Phys. Rev. Lett. **31**, 656 (1973).¹¹H. Fritzsche and J. D. Jackson, Phys. Lett. **66B**, 365 (1977).¹²H. J. Lipkin, in *Orbis Scientiae, Deeper Pathways in High Energy Physics, Coral Gables, 1977*, edited by B. Kursunoglu, A. Perlmutter, and L. F. Scott (Plenum, New York, 1977), p. 567.¹³After the original version of this paper was submitted for publication a paper by J. F. Donoghue and Barry R. Holstein [Massachusetts Institute of Technology Report No. CTP-779 (to be published)] was received including a discussion of final-state interactions with a point of view similar to ours, but a very different analysis of the scalar meson resonances and very different conclusions.

Decay $J/\psi \rightarrow 3\gamma$ and a Search for the η_c

R. Partridge, C. Peck, and F. Porter

Physics Department, California Institute of Technology, Pasadena, California 91125

and

W. Kollman,^(a) M. Richardson, K. Strauch, and K. Wacker*Lyman Laboratory of Physics, Harvard University, Cambridge, Massachusetts 02138*

and

D. Aschman, T. Burnett,^(b) M. Cavalli-Sforza, D. Coyne, and H. Sadrozinski*Physics Department, Princeton University, Princeton, New Jersey 08540*

and

E. Bloom, F. Bulos, R. Chestnut, J. Gaiser, G. Godfrey, C. Kiesling, and M. Oreglia

Stanford Linear Accelerator Center, Stanford University, Stanford, California 94305

and

R. Hofstadter, I. Kirkbride, H. Kolanoski, A. Liberman,^(c) J. O'Reilly, and J. Tompkins*Physics Department and High Energy Physics Laboratory, Stanford University, Stanford, California 94305*

(Received 17 December 1979)

The decay J/ψ into 3γ final states has been studied. No evidence is found for the existence of the $X(2.83)$ or any heavy narrow state (e.g., the η_c) decaying into two photons. Upper limits are given on the branching ratio $J/\psi \rightarrow \eta_c$, $\eta_c \rightarrow 2\gamma$ for η_c masses in the 2.7–3.0-GeV region. In addition, the branching ratios $J/\psi \rightarrow \gamma\eta, \gamma\eta'$ are measured. It is found that the η' branching ratio is higher than previously reported.

Using a nonmagnetic neutral-particle detector, the "Crystal Ball," we are studying the e^+e^- annihilation process with the SPEAR storage ring at various energies. We report here our results for the decay of the J/ψ into 3γ final states with the J/ψ produced directly via $e^+e^- \rightarrow J/\psi$, and indirectly via $e^+e^- \rightarrow \psi' \rightarrow \pi^+\pi^- J/\psi$.

The three-photon final states of the J/ψ can be reached through either $J/\psi \rightarrow \gamma X$, where X is any state which decays into two γ 's (e.g., π^0, η, η'), or $J/\psi \rightarrow 3\gamma$ (direct). When the J/ψ is produced directly, the quantum electrodynamics (QED) reaction $e^+e^- \rightarrow 3\gamma$ also contributes. There is no such contribution when the J/ψ originates from

ψ' decays.

The η_c , which is the 1S_0 state of charmonium predicted by charmonium models,¹ is a further possibility for the X . Evidence for a state at a mass of 2.83 GeV has been reported by another experiment² in a study of the reaction $e^+e^- \rightarrow J/\psi + 3\gamma$. However, the strength of the signal at the reported mass is inconsistent with the prediction of these models and has posed serious difficulty to their advocates.

The Crystal Ball is shown schematically in Fig. 1. The main components are the following:

(1) The ball, consisting of two hemispherical shells of NaI(Tl) 16 radiation lengths thick, cen-

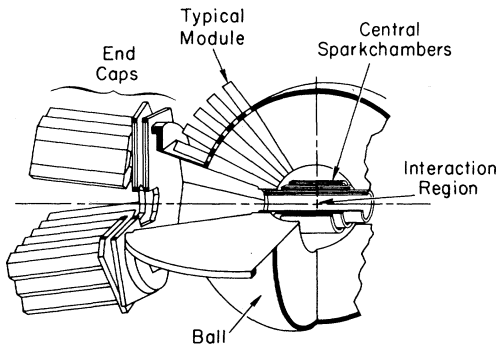


FIG. 1. Schematic of Crystal Ball detector.

tered around the interaction region and covering 94% of 4π sr. Each hemisphere is divided into 336 modules. Each module has the shape of a truncated pyramid with a triangular cross section, is optically separated from its neighbors, and is viewed by a phototube.

(2) Central cylindrical wire chambers, each consisting of a proportional chamber sandwiched between two magnetostrictive-readout spark chambers. The assembly surrounds a thin wall (1.5 mm) Al beam pipe. The three chambers cover 94%, 80%, and 71% of 4π sr.

(3) End caps, consisting of planar magnetostrictive-readout spark chambers followed by individually sealed hexagonal NaI(Tl) modules 20 radiation lengths thick. These end caps increase the solid-angle coverage to 98% of 4π sr.

A photon deposits all its energy in a cluster of several modules leaving no hits in the wire chambers. The direction of such a "neutral track" is obtained by joining the center of the interaction region to the shower center determined by shower pattern methods. We have achieved, in the Crystal Ball, an angular resolution for photons of $\sigma = 2^\circ$ and an energy resolution for photons and electrons of $(\sigma/E) = 2.8\%/E^{1/4}$. Bloom,³ Godfrey,⁴ Chan,⁴ O'Reilly,⁵ and Kirkbride⁵ contain detailed descriptions of the detector, the electronics and trigger, and calibration procedures.

Our results are based on an integrated luminosity of 1700 nb^{-1} at the ψ' ($\sim 8 \times 10^5 \psi'$), and 327 nb^{-1} at the J/ψ ($\sim 9 \times 10^5 J/\psi$). The experimental trigger used in the present study is a total energy trigger which requires $> 900 \text{ MeV}$ deposited in the ball. Since the full mass of the J/ψ is deposited by the three photons in the ball, this trigger alone is fully efficient.

For the selection of 3γ events from direct J/ψ

production, we require three neutral tracks with a total energy of $> 2.7 \text{ GeV}$ in the ball and $\leq 25 \text{ MeV}$ in the endcaps. To enhance charged-particle tagging efficiency, we require $|\cos\theta_\gamma| \leq 0.8$ for each photon where θ_γ is the photon polar angle with respect to the beam. We also require a momentum imbalance of $\leq 500 \text{ MeV}$ and for each photon an energy $E_\gamma > 20 \text{ MeV}$. A total of 865 events fulfill these criteria.

In order to avoid problems with overlapping showers we require $\cos\theta_{\gamma\gamma} \leq 0.85$ where $\theta_{\gamma\gamma}$ is the angle between any two photons. This cut also eliminates most events from $J/\psi \rightarrow \gamma\pi^0$, and hence the present analysis cannot give any results for this reaction.

The main source of background is the decay $J/\psi \rightarrow \gamma\pi^0\pi^0$ where the two decay photons from a π^0 overlap to produce a single merged shower with an unusually large lateral spread. Events with one or more such showers are rejected using a lateral shower-distribution algorithm developed with the help of Monte Carlo calculations.

Each surviving event is subjected to a four-constraint kinematic fit. The final sample of 405 events is estimated to contain approximately fourteen background events. Of these, approximately three are due to radiative Bhabha scattering where neither electron is detected by the spark chambers. The remaining approximately eleven events come from $\gamma\pi^0\pi^0$ final states which pass our selection criteria; their distribution in the Dalitz plot is nearly uniform.

For the selection of events where the J/ψ originates from ψ' decay, we require two charged particles, and three photons with an invariant mass $2.82 < M_{\gamma\gamma\gamma} < 3.25 \text{ GeV}$, and each photon with an energy $E_\gamma > 20 \text{ MeV}$. In order to increase the acceptance, we relax the angular limits to $|\cos\theta_\gamma| < 0.85$ and $\cos\theta_{\gamma\gamma} < 0.90$. The rest of the procedure remains the same except that the remaining events undergo a three-constraint fit with $M_{\gamma\gamma\gamma}$ constrained at the J/ψ mass. 29 events remain.

From each final sample we obtain a Dalitz plot of the highest and lowest invariant mass squared, $(M_{\gamma\gamma})_{\text{low}}^2$ and $(M_{\gamma\gamma})_{\text{high}}^2$. Figures 2 and 3 show such plots for directly and indirectly produced J/ψ . Histograms of $(M_{\gamma\gamma})_{\text{low}}$ and $(M_{\gamma\gamma})_{\text{high}}$ are also shown in Figs. 4(a) and 4(b) for J/ψ produced directly. η and η' peaks stand out clearly in Fig. 4(a). On the basis of the results of Ref. 2 and our mass resolution ($\sim 30 \text{ MeV}$), a peak containing 46 ± 19 events above background is expected in the two bins containing the $X(2.83)$ in Fig. 4(b).

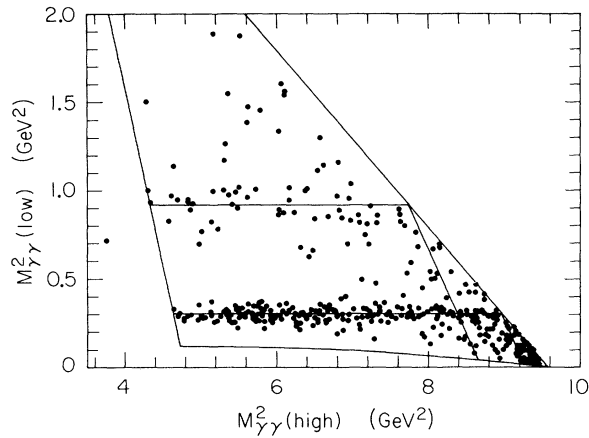


FIG. 2. Dalitz plot of $J/\psi \rightarrow 3\gamma$.

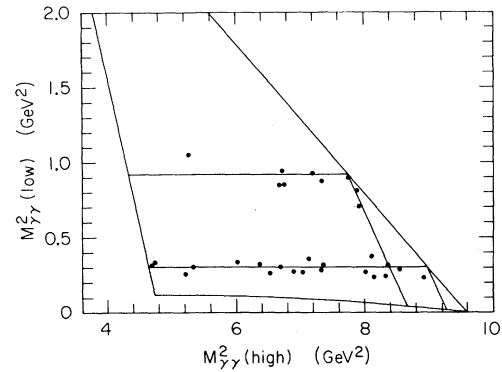


FIG. 3. Dalitz plot of $\psi' \rightarrow J/\psi \pi^+ \pi^-$, $J/\psi \rightarrow 3\gamma$.

We see no such peak.

In order to find the contributions from individual reactions in $J/\psi \rightarrow \gamma X$, $X \rightarrow 2\gamma$, a two-dimensional maximum-likelihood fit to the Dalitz plot was carried out. For J/ψ produced directly, events from each individual reaction were simulated in the detector by Monte Carlo shower calculations using a $(1 + \cos^2\theta)$ distribution for the monochromatic photon. For direct 3γ and QED, the matrix elements given in Pelaquier and Renard⁶ and Berends and Gastmans⁷ were used. The energy resolution as well as photon-conversion corrections were introduced into the Monte Carlo

calculations. The events were then subjected to the same selection and analysis as the data, yielding a Dalitz-plot density and an overall acceptance for each reaction. These were used in the Dalitz-plot fit leaving only the individual numbers of events from the various reactions as free parameters. Such fits have been carried out for several values of the η_c mass, and upper limits obtained at each mass. In addition to the fit we have also calculated the absolute contribution from QED at the J/ψ and $\psi''(3770)$. The calculations were found to be in very good agreement with the data at the ψ'' (where QED is the only source for the 3γ final state), and with the QED contribution obtained from the fit at J/ψ .

From the fit to the Dalitz plot we obtain an upper limit for the branching-ratio product at an X mass of 2.83 GeV:

$$R(J/\psi \rightarrow \gamma X) \times R(X \rightarrow 2\gamma)$$

$$< 2.2 \times 10^{-5} \text{ (90\% confidence level).}$$

Figure 5 shows this product as a function of η_c mass, and a theoretical prediction from Appelquist *et al.*⁸ for comparison. Reference 8 also

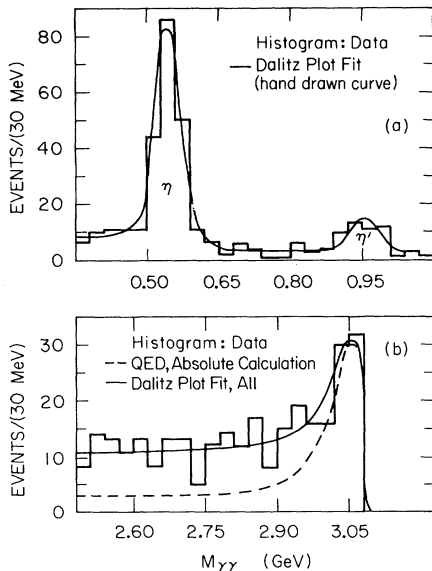


FIG. 4. (a) Histogram of $(M_{\gamma\gamma})_{low}$, $J/\psi \rightarrow 3\gamma$. (b) Histogram of $(M_{\gamma\gamma})_{high}$, $J/\psi \rightarrow 3\gamma$.

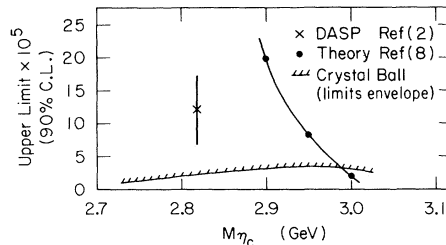


FIG. 5. Upper limits: $R(J/\psi \rightarrow \gamma \eta_c) \times R(\eta_c \rightarrow 2\gamma)$.

contains a discussion of the difficulty posed by an η_c mass of 2.83 GeV.

Since the only significant contributions found were from η , η' , and QED, a fit to the Dalitz plot has been carried out using these only. This fit yields the following branching ratios⁹: $R(J/\psi \rightarrow \gamma\eta) = (1.17 \pm 0.17) \times 10^{-3}$, $R(J/\psi \rightarrow \gamma\eta') = (6.87 \pm 1.71) \times 10^{-3}$. The first is in good agreement with previous measurements.^{2,10} The second is higher than earlier results.^{2,11} Our value of 5.88 ± 1.46 for the ratio of the two decay rates $\rho \equiv R(J/\psi \rightarrow \gamma\eta')/R(J/\psi \rightarrow \gamma\eta)$ can be compared to earlier experimental results¹⁰ $\rho = 1.8 \pm 0.8$, $\rho = 2.8 \pm 2.2$ (derived from Ref. 2), and the theoretical value¹² $\rho \approx 3.9$.

For the 3γ decay of J/ψ obtained from ψ' , all events in the Dalitz plot (Fig. 3) are in the η and η' mass bands. In particular, there are no contributions from $X(2.83)$. As stated before, this reaction is free from QED. The Dalitz plot was therefore fitted with only η , η' , $X(2.83)$, and direct 3γ . Our present knowledge of the hadronic showers in the ball does not allow us to calculate reliably the efficiency of event selection. We therefore normalized the branching ratios by comparing the total number of $\eta + \eta'$ from this method with that from J/ψ produced directly. This procedure is justified because the selection inefficiencies due to the charged particles should be independent of the 3γ final state.

Since the sum of the η , η' is used in the normalization, we can give only the value for the ratio ρ defined above. We find $\rho = 10.01 \pm 4.1$.

The fit to the Dalitz plot gives no events from $X(2.83)$. Using the normalization above, we obtain an upper limit on the branching-ratio product

$$R(J/\psi \rightarrow \gamma X(2.83)) \times R(X(2.83) \rightarrow 2\gamma) < 1.0 \times 10^{-4} \text{ (90\% confidence level).}$$

Also, no contribution from direct 3γ decay is required by the fit and we obtain the upper limit $R(J/\psi \rightarrow \text{direct } 3\gamma) < 5.5 \times 10^{-5}$ (90% confidence level). For the convenience of the reader, the results appearing in various parts of the text are compiled in Table I.

A complex detector such as the Crystal Ball could not have been designed, built, and operated without considerable technical and administrative help from many individuals. Our sincere thanks go to all of them even though space limits us to naming the following only: A Baumgarten and J. Broeder [Stanford Linear Accelerator Center

TABLE I. Branching ratios $J/\psi \rightarrow 3\gamma$.

Channel	Branching ratio
$J/\psi \rightarrow \gamma\eta$	$(1.17 \pm 0.17) \times 10^{-3}$
$J/\psi \rightarrow \gamma\eta'$	$(6.87 \pm 1.71) \times 10^{-3}$
$(J/\psi \rightarrow \gamma\eta')/(J/\psi \rightarrow \gamma\eta)$	(5.88 ± 1.46)
$J/\psi \rightarrow 3\gamma$ (direct) ^a	$< 5.5 \times 10^{-5}$
$J/\psi \rightarrow \gamma X(2.83), X \rightarrow 2\gamma$	$< 2.2 \times 10^{-5}$

^aHere J/ψ is obtained from the decay $\psi' \rightarrow J/\psi \pi^+ \pi^-$.

(SLAC)]; R. Parks [High Energy Physics Laboratory (HEPL), Stanford University]. B. Beron and E. B. Hughes (HEPL, Stanford University) were valued participants in the early phases of the program.

This work was supported by the U. S. Department of Energy under Contracts No. DE-AC-3-76SF00515, No. EY-76-C02-3064, and No. EY-76-C03-0068, and by the National Science Foundation Contracts No. PHY78-00967, No. PHY78-07343, and No. PHY75-22980. Support for individuals came from the listed institutions together with NATO-Fellowship-West Germany, Chaim Weizmann Fellowship, and the Sloan Foundation.

^(a)Present address: Wentorfer Strasse 149, 2050 Hamburg, West Germany.

^(b)Permanent address: Physics Department, University of Washington, Seattle, Washington 98195.

^(c)Schlumberger-Doll Research Center, Ridgefield, Connecticut 06877.

¹See for instance E. Eichten *et al.*, Phys. Rev. D **17**, 3090 (1978).

²W. Braunschweig *et al.*, Phys. Lett. **67B**, 1243 (1978).

³E. D. Bloom, in Proceedings of the XIVth Rencontre de Moriond, Moriond, 1979 (to be published).

⁴G. Godfrey, in Proceedings of the IEEE Conference, San Francisco, October 1977 (unpublished); Y. Chan *et al.*, IEEE Trans. Nucl. Sci. **25**, 333 (1978).

⁵J. O'Reilly, in Proceedings of the Fifth Conference on Applications of Small Accelerators, Denton, Texas, 1978 (unpublished); I. Kirkbride *et al.*, IEEE Trans. Nucl. Sci. **26**, 1535 (1979).

⁶E. Pelaquier and F. M. Renard, Nuovo Cimento **32A**, 421 (1976).

⁷F. A. Berends and R. Gastmans, Nucl. Phys. **B61**, 414 (1973).

⁸T. Appelquist *et al.*, Annu. Rev. Nucl. Part. Sci. **28**, 387-499 (1978).

⁹We use the following branching ratios for $\eta, \eta' \rightarrow 2\gamma$:

$$R(\eta \rightarrow 2\gamma) = (38.0 \pm 1.0) \times 10^{-2},$$

$$R(\eta' \rightarrow 2\gamma) = (1.9 \pm 0.3) \times 10^{-2}.$$

¹⁰W. Bartel *et al.*, Phys. Lett. **66B**, 489 (1977).

¹¹W. Bartel *et al.*, Phys. Lett. **64B**, 483 (1976).

¹²H. Fritzsche and J. D. Jackson, Phys. Lett. **66B**, 365 (1977).

Deformation Dependence of the Pairing Strength Investigated by Electrofission of ^{182,184,186}W

W. Günther, R. Haag, K. Huber, U. Kneissl, H. Krieger, H. J. Maier, and H. Ströher
Institut für Kernphysik, Strahlenzentrum der Universität Giessen, D-6300 Giessen, West Germany, and
II. Physikalisches Institut der Universität, Giessen D-6300 Giessen, West Germany, and
Tandemlabor, Ludwig-Maximilian Universität München, D-8000 München, West Germany

(Received 22 October 1979)

The electroinduced fission of ^{182,184,186}W has been investigated in the energy range from 35 to 55 MeV. The fission barriers, estimated by a statistical-model analysis of the measured cross sections, are compared with theoretical predictions and are only consistent with the assumption of a constant pairing strength.

The aim of this study was the investigation of the deformation dependence of the pairing strength G by comparing experimentally determined fission barriers with calculated potential-energy surfaces (PES). The pairing strength is mostly supposed to be constant, but there have been both theoretical and experimental suggestions that it might be a function of the nuclear surface area.^{1,2}

Mosel³ has performed Strutinsky-type calculations of potential-energy surfaces within the two-center shell model in the mass region $180 \leq A \leq 212$, assuming both a constant and a surface-dependent pairing strength.

Figure 1 shows the calculated fission barriers as a function of the neutron number of the fissioning nucleus. There are two features to be noticed. First there is a strong increase of the fission barriers in the lead region, which is mainly caused by the ground-state shell corrections. Recently this increase was excellently confirmed by electrofission experiments.^{4,5} On the other hand the calculated barriers for lighter elements, e.g., the tungsten isotopes ($Z=74$), strongly depend on the assumed deformation dependence of the pairing strength ($G = \text{const}$ or $G \sim S$). The reason for this is the larger saddle-point construc-

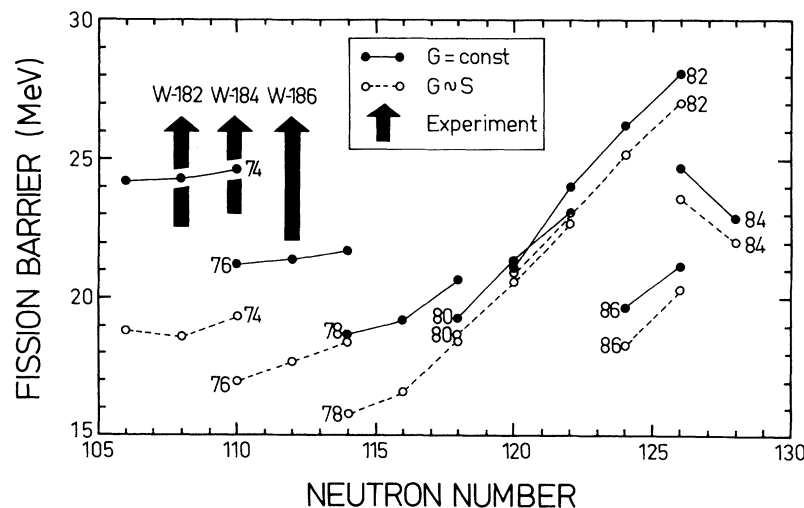


FIG. 1. Calculated fission barriers (Ref. 3) (full lines, $G = \text{const}$; dashed lines, $G \sim S$) and limits deduced from our experiments on ^{182,184,186}W.